BUBBLE FORMATION AND GROWTH

Study of the Boundary Conditions at a Liquid-Vapor Interface through Irreversible Thermodynamics

by

Walter J. Bornhorst
and
George N. Hatsopoulos

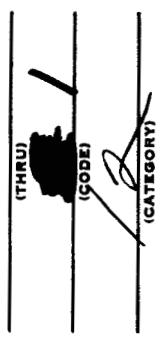

Quarterly Progress Report

March - May, 1966

for

National Aeronautics and Space Administration
George C. Marshall Space Flight Center
Huntsville, Alabama
Attn: PR-EC
Contract No. NAS 8-20013
Control No. 1-5-52-01122-01 (1F)

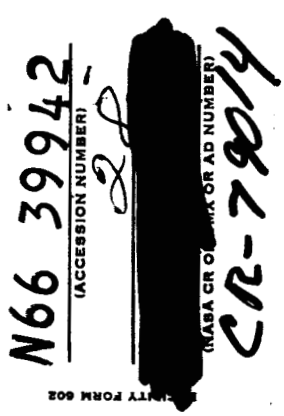

June 1966

Department of Mechanical Engineering
Massachusetts Institute of Technology

BUBBLE GROWTH CALCULATION WITHOUT NEGLECT OF INTERFACIAL DISCONTINUITIES[1]

W. J. Bornhorst

Assistant Professor of Mechanical Engineering
Massachusetts Institute of Technology, Cambridge, Mass.

G. N. Hatsopoulos

Senior Lecturer of Mechanical Engineering
Massachusetts Institute of Technology, Cambridge, Mass.

ABSTRACT

The object of this theoretical investigation is to determine the importance of the nonequilibrium region, which exists at the bubble wall, on the growth of a vapor bubble. All previous investigators concerned with bubble growth have completely neglected this nonequilibrium effect. In the previous paper Bornhorst and Hatsopoulos investigated the phase change problem, and the results which were obtained are applied here to solve the special problem of vapor bubble growth.

The results are presented in terms of a two-parameter set of curves. These results show that for pressures where experimental results are available, the nonequilibrium effects are within experimental error; however, for pressures which are somewhat lower, the nonequilibrium effects become very important.

1. INTRODUCTION

When a vapor bubble grows, material passes from one phase to another at a net finite rate near the bubble wall. A very thin but finite nonequilibrium region must exist at the interface to allow for this phase

---

[1]This work was sponsored by NASA contract NAS8-20013.

transition. In this nonequilibrium region thermodynamic properties, such as temperature and chemical potential, lose their meaning, as also does the Fourier heat conduction law along with other continuum equations. We should not expect a finite rate of energy or mass to pass through this nonequilibrium region without a corresponding drop in temperature and chemical potential. Subsequently, we shall speak of these changes as discontinuities, realizing, however, that they really result from a gap in the temperature and chemical potential profiles.

In order to connect the bulk conservation equations across the nonequilibrium region, it is necessary to have a set of equations which relate the interfacial discontinuities to the flux of mass and energy across the interface. This set of equations, which will be used here, was described in the previous paper by Bornhorst and Hatsopoulos [1].

In all previous bubble growth analyses, the effects of this non-equilibrium region at the bubble wall have been completely neglected. In other words, it has always been assumed that the temperature and chemical potential are equal in the liquid and vapor phases at the interface. This assumption is equivalent to assuming that the pressure and temperature at the interface are related by saturation conditions. Subsequently, we shall refer to this assumption as the equilibrium assumption. The purpose of this paper is to obtain equations for bubble growth rates without making this assumption. The results thus obtained show that the equilibrium assumption causes large errors for bubble growth rates at low pressures.

The first solution for the problem of bubble growth was reported by Rayleigh.[2] In his analysis he considered only dynamic effects and completely neglected the cooling effect of evaporation. His conclusion was that bubbles grow at a constant velocity. Later Plesset and Zwick[3] and others[4, 5] obtained asymptotic solutions (valid for sufficiently large values of the radius R) which completely neglected nonequilibrium effects but included the cooling effect of evaporation. Their conclusion was that the cooling effect is very important and that the bubble wall velocity is proportional to the inverse square root of time. This conclusion is in agreement with experimental bubble growth measurements made by Dergarabedian.[6] These measurements do not justify the equilibrium assumption for the general case of bubble growth because the experimental conditions of Dergarabedian's experiments were such that the nonequilibrium effects were unimportant for his specific tests.

2. DERIVATION OF BUBBLE GROWTH EQUATION

The goal of the present analysis is to reduce the appropriate conservation equations to a single differential equation for the bubble wall velocity $\dot{R}$. This solution should be at least approximately valid for both early and late bubble growth.

2.1 Rayleigh Equation

The momentum equation for a spherically symmetric flow of an incompressible Newtonian fluid with no body forces is

$$\frac{\partial u}{\partial t} + u \frac{\partial u}{\partial r} = - \frac{1}{\rho_f} \frac{dP}{dr} + \frac{\mu}{\rho_f} \nabla^2 u , \qquad (1)$$

where u denotes the radial liquid velocity. With these assumptions the continuity equation gives

$$ur^2 = f_1(t) \ , \tag{2}$$

where $f_1(t)$ represents an arbitrary function of time which can be evaluated at the bubble wall by considering an overall mass balance for the bubble. From this mass balance we find that

$$u = \dot{R} \frac{R^2}{r^2} \ , \tag{3}$$

where we have assumed that

$$\rho_g / \rho_f << 1 \ , \tag{4}$$

and also that

$$\frac{d}{dt} (4/3 \pi R^3 \rho_g) = 4\pi \rho_g R^2 \dot{R} \ . \tag{5}$$

Assumption (4) is certainly very good especially at low pressures, and the second assumption can be physically justified since the bubble radius changes orders of magnitude while the vapor density variations are relatively small.[3] The expression for u given by (3) can be substituted into (7), and since the viscous term is identically equal to zero, the resulting equation can be integrated from the bubble wall out to infinity. If we also include the pressure drop across the interface due to surface tension, we obtain the familiar Rayleigh equation

$$\frac{P_g - P_\infty}{\rho_f} = \frac{2\sigma_s}{R\rho_f} + R \frac{d\dot{R}}{dt} + 3/2 \dot{R}^2 \ . \tag{6}$$

2.2 Energy Equation

The energy equation appropriate for the liquid phase is

$$\frac{\partial T}{\partial t} + \frac{R^2}{r^2}\dot{R}\frac{\partial T}{\partial r} = \alpha \frac{1}{r^2}\frac{\partial}{\partial r}\left(r^2 \frac{\partial T}{\partial r}\right), \tag{7}$$

where we made use of equation (3) to express the convection velocity u in terms of $\dot{R}$. The boundary condition at the bubble wall is obtained by applying the first law to a control volume consisting of the vapor bubble

$$k_f\left(\frac{\partial T}{\partial r}\right)_{r=R} = \rho_g h_{fg} \dot{R}, \tag{8}$$

where we have dropped small terms due to compressibility effects and temperature changes in the vapor. Physically Equation (8) states that the temperature slope in the liquid must be such to supply the required energy to evaporate the liquid.

To solve Equation (7) in conjunction with (8), we employ an approximate integral technique developed by Murdock.[7] This method consists of assuming a second-order temperature distribution in the liquid thermal boundary layer. The boundary layer thickness is determined by requiring the integrated distribution to satisfy the energy equation. The details of this analysis along with a discussion concerning the validity of the integral approximation is given in Appendix A. The result which is shown to be valid for low pressures is

$$\dot{R} = \frac{2k_b^2 R^2}{R^3 - R_o^3}(T_\infty - T_{fi})^2 \tag{9}$$

where T_{fi} is the temperature of the liquid at the bubble wall and k_b is a function of fluid properties defined by

$$k_b = \frac{k_f}{\rho_g h_{fg} \sqrt{\alpha}} \quad . \tag{10}$$

2.3 Irreversible-Flow Equations

In order to combine Equations (6) and (9), we need a relation between T_{gi} and P_g. If we were to admit thermodynamic equilibrium at the bubble wall, such a relation would be given by the Clapeyron equation; however, here we shall avoid the equilibrium assumption by employing Equations (20) and (21) from the previous paper by Bornhorst and Hatsopoulos.[1] These equations may be written as

$$J_u = J_i \left(h_g \frac{K h_{fg}}{K + 1}\right) - L_k \frac{\delta T}{T^2} \quad , \tag{11}$$

and

$$J_i / L_{ii} = \frac{K}{(K + 1)} \frac{h_{fg}}{T^2} \delta T - \frac{1}{T} v_{fg} \delta_f P \tag{12}$$

where J_u and J_i denote the energy and mass flux, respectively, K, L_k, and L_{ii} represent transport coefficients, and the defining equations for δT and $\delta_f P$ are

$$\delta T \equiv T_{gi} - T_{fi} \tag{13}$$

and

$$\delta_f P \equiv P_f - P_{fs} \tag{14}$$

where P_f is the actual pressure of the liquid at the interface, and P_{fs} is the saturation pressure at T_{fi} and the radius R.

Rewriting Equation (12) in a more convenient form and substituting for J_i in terms of $\dot{R}$ (see Equation (5)), we obtain

$$\dot{R} = \frac{-L_{ii} P v_{fg}}{\rho_g T} \left[\frac{-K}{K+1} \frac{h_{fg}}{P v_{fg}} \frac{\delta T}{T} + \frac{\delta_f P}{P} \right] . \tag{15}$$

If we assume that the kinetic theory expressions give the correct order of magnitude for $K/(K+1)$ and L_k, we can show that the first term in the brackets is small compared to the second. This is accomplished in Appendix B by taking into account the energy supplied to the vapor. With this simplification Equation (15) becomes

$$\dot{R} = - \frac{2 \sigma_c}{(2 - \sigma_c)} \frac{P}{\rho_g (2\pi \bar{R} T)^{1/2}} \frac{\delta_f P}{P} , \tag{16}$$

where L_{ii} was replaced by another transport coefficient σ_c defined by the relation

$$\frac{2 \sigma_c}{2 - \sigma_c} = \frac{(2\pi \bar{R} T)^{1/2} v_{fg} L_{ii}}{T} . \tag{17}$$

The quantity σ_c becomes identical to the condensation coefficient if the kinetic theory results, given in section 4 of the previous paper by Bornhorst and Hatsopoulos, are assumed correct.

From the definition of $\delta_f P$ (Equation (14)) and the Clapeyron relation, we can obtain

$$\sigma_f P = (P_g - P_\infty) + \frac{\rho_g h_{fg}}{T} \left[(T_\infty - T_{fi}) - \Delta T_s\right] , \qquad (18)$$

where ΔT_s is the superheat of the liquid at infinity. It should be noted that the use of the Clapeyron relation here implies nothing about the actual equilibrium of the liquid-vapor system. Equations (16) and (18) can be combined to yield

$$\dot{R} = \frac{-2\sigma_c}{(2-\sigma_c)} \frac{1}{(2\pi \bar{R} T)^{1/2} \rho_g} \left[(P_g - P_\infty) + \frac{\rho_g h_{fg}}{T_\infty} (T_\infty - T_{fi} - \Delta T_s) \right] . \qquad (19)$$

2.4 Final Differential Equation for Bubble Growth

The final differential equation is obtained from (19) by substituting for $(P_g - P_\infty)$ from Equation (6) and for $(T_\infty - T_{fi})$ from Equation (9). The result is

$$\dot{R} = \frac{2 k_o^2 R^2}{(R^3 - R_o^3)} \left[\Delta T_s - \underbrace{\frac{T_o 2 \sigma_s}{\rho_g h_{fg} R}}_{\text{Surface Tension}} - \underbrace{\frac{T_o (2\pi \bar{R} T)^{1/2} \dot{R}}{h_{fg} \left(\frac{2\sigma_c}{2-\sigma_c}\right)}}_{\text{Nonequilibrium Effect}} - \underbrace{\frac{T_o \rho_f}{h_{fg} \rho_g} \left(R\dot{R} \frac{d\dot{R}}{dR} + 3/2 \dot{R}^2\right)}_{\text{Liquid Inertia}} \right]^2 . \qquad (20)$$

The physical interpretation of Equation (20) is that the potential driving temperature difference ΔT_s is diminished by surface tension, nonequilibrium effects, and finally by liquid inertia effects.

Equation (20) can be numerically integrated; however, before proceeding to this it is beneficial to nondimensionlize this equation. The characteristic length is chosen to be the unstable equilibrium radius R_o, and the characteristic bubble wall velocity is taken to be the maximum velocity the bubble wall would attain if nonequilbrium effects and liquid

inertia effects were identically zero. We shall call this bubble wall velocity $\dot{R}_o$. The defining equations for R_o, $\dot{R}_o$, and the corresponding dimensionless quantities $\hat{R}$ and $\hat{\dot{R}}$ are

$$R_o \equiv \frac{2 T_o \sigma_s}{\rho_g h_{fg} \Delta T_s} \quad , \quad \dot{R}_o \equiv \frac{2 k_b^2 \Delta T_s}{R_o(3 + 2\sqrt{3})} \quad , \tag{21}$$

and

$$\hat{R} \equiv R/R_o \quad , \quad \hat{\dot{R}} \equiv \dot{R}/\dot{R}_o \quad . \tag{22}$$

Introducing these definitions in Equation (20), we obtain

$$\dot{R} = \frac{(3 + 2\sqrt{3})\,\hat{R}^2}{(\hat{R}^3 - 1)} \left[1 - \frac{1}{\hat{R}} - \beta \hat{\dot{R}} - \frac{M}{(3 + 2\sqrt{3})^2} (\hat{\dot{R}}\hat{R} + 3/2\, \hat{\dot{R}}) \right]^2 , \tag{23}$$

where β and M are functions of the fluid properties and the initial conditions. The defining equations for β and M are

$$\beta \equiv \frac{\rho_g k_b (2\pi \bar{R} T)^{1/2} (2 - \sigma_c) \Delta T_s^2}{\sigma_s (3 + 2\sqrt{3})\, 2\sigma_c} \quad , \tag{24}$$

and

$$M \equiv \frac{\rho_f k_f^4 \Delta T_s^5}{\rho_g^3 h_{fg}^3 \alpha^2 T \sigma_s^2} \quad . \tag{25}$$

It is readily seen that β is a measure of the nonequilibrium effect while M is a measure of the liquid inertia effect.

Equation (23) was numerically integrated on a computer for various values of the fluid parameters β and M. The results are presented in the next section.

3. PRESENTATION OF BUBBLE GROWTH RESULTS

3.1 Explanation of Graphs

Values for the fluid parameters β and M for various fluids are plotted in Figs. 1 and 2 against the reduced temperature T_R. The reduced temperature T_R is the ratio of the saturation temperature T_o to the critical temperature T_c. The strong dependence of β and M on the saturation temperature and, therefore, also on the external pressure P_∞ should be noted. This means that the nonequilibrium effects which vary directly with β and indirectly with M are also strongly dependent on the temperature T_o and external pressure P_∞. As is seen from Figs. 1 and 2 the nonequilibrium and momentum effects increase with decreasing pressure.

Figs. 3 through 5 show plots of the dimensionless bubble wall velocity $\dot{R}$ versus the dimensionless bubble radius R. Each figure is for a fixed value of M while β is varied from zero to a reasonable value corresponding to the particular value of M.

The curve labeled "β equal to zero" corresponds to the solution one would obtain if thermodynamic equilibrium were assumed. Thus the nonequilibrium effect is the difference between this curve and the curve with β corresponding to the case of interest.

The curve labeled "asymptotic solution ($\beta = 0$, $M = 0$)" corresponds to the solution obtained by several authors [3, 4, 5] valid for late bubble growth. It can be seen from Figs. 3 through 5 that the asymptotic solution becomes valid only at very large radii, especially for the large values of M.

On each figure a table is given which relates the particular values of β and M to a specific operating condition for a specific liquid. Since M is not a function of the condensation coefficient σ_c, we may tag a value of σ_c to each value of β for a given operating condition.

The linear requirement which can be obtained from Equation (16), and the definition for $\dot{R}$ and β is that

$$\frac{\delta_f P}{P} = \hat{\dot{R}} \beta \left(\frac{\rho_g h_{fg}}{P_\infty}\right) \left(\frac{\Delta T_s}{T}\right) << 1$$

The maximum value of $\delta_f P/P$ for the cases considered in Figs. 3, 4, and 5 is listed on each figure. All the cases are seen to be approximately linear except for nitrogen where $\delta_f P/P$ may be as large as 0.6. By reducing the superheat ΔT_s and increasing the external pressure P_∞, we can get cases for nitrogen which are linear and still exhibit important nonequilibrium effects.

3.2 Significance of Results

The results obtained clearly indicate the importance of the nonequilibrium effects by the spread of the curves on Figs. 3 through 5. It should be noted that the nonequilibrium and momentum effects decay faster with bubble radius for the smaller values of β and M. The effect of both β and M is to greatly increase the extent of what has been called the initial bubble growth, that is, the growth up to the point where the asymptotic solution becomes reasonably accurate.

In order to illustrate the points mentioned above, we shall consider the example of a vapor bubble growing in water at an external pressure P_∞ equal to 0.178 psi. The corresponding saturation temperature

T_o is found to be 510°R. For this value of T_o and a value of the condensation coefficient σ_c equal to unity, we find from Fig. 1 a value of $\beta/\Delta T_s^2$ equal to 0.01 and from Fig. 2 a value of $M/(\Delta T_s)^5$ approximately equal to 10^{-2}. If we choose to take ΔT_s equal to 10°F, we then obtain a value for β of 1.0 and a value for M of 10^3. Since Fig. 4 corresponds to M equal to 10^3, the curves on this figure represent the case at hand. The different values of β correspond to various values of the condensation coefficient σ_c. For the example considered, Fig. 6 shows the real bubble velocity (ft/sec) versus the real bubble radius (ft) for various values of σ_c. For this case we conclude that the nonequilibrium effects are very important for a large portion of the bubble's growth.

3.3 Suggested Experiments

All existing experimental data on bubble growth rates correspond to such low values of β and M that the nonequilibrium effects are unimportant in these experiments. In order to check the present theory, bubble growth measurements are needed at low pressures with the corresponding high values of β and M.

Since bubble growth rates have been found to be such a strong function of β, and therefore also of σ_c, it is suggested that σ_c be measured from bubble growth experiments performed at low pressures. One obvious advantage of this type of experiment is the elimination of the contamination problems which seriously plagued most previous attempts to measure σ_c, especially those for the non-metals such as water.

REFERENCES

1. Bornhorst, W. J. and Hatsopoulos, G. N., J. Appl. Mech. (To be published).

2. Rayleigh, Phil. Mag. 34, 94 (1917).

3. Plesset, M. S. and Zwick, S. A., J. Appl. Phys. 25, 493 (1954).

4. Forster, H. K. and Zuber, N., J. Appl. Phys. 25, 475 (1954).

5. Scriven, L. E., Chem. Eng. Sci., 10, 1, (1959).

6. Dergarabedian, P., J. of Fluid Mech., 9, 39 (1960).

7. Murdock, J., Internal Report in Mechanical Engineering Department, Mass. Inst. of Tech., 1965.

APPENDIX A

Energy Integral Technique

Most of the concepts in this appendix were taken from a report by Murdock. [7]

The object is to solve

$$\frac{\partial T}{\partial t} + \frac{R^2}{r^2}\dot{R}\frac{\partial T}{\partial r} = \alpha \frac{1}{r^2}\frac{\partial}{\partial r}\left(r^2 \frac{\partial T}{\partial r}\right), \qquad \text{(A-1)}$$

with the boundary condition at the bubble wall

$$k_f \left(\frac{\partial T}{\partial r}\right)_{r=R_+} = \rho_g h_{fg} \dot{R}, \qquad \text{(A-2)}$$

where the notation is the same as used in the body of this paper.

The other boundary condition far from the bubble wall is

$$p(\infty, t) = P_\infty ,$$

and the initial conditions are

$$P(r, 0) = P_\infty \quad ,$$

and

$$T(r, 0) = T_\infty \quad . \tag{A-3}$$

A thermal boundary layer of thickness δ is assumed to exist in the liquid outside the vapor bubble. The temperature profile assumed in the boundary layer is

$$T - T_{fi} = (T_\infty - T_{fi}) \left[\frac{2(r - R)}{\delta} - \left(\frac{r - R}{\delta}\right)^2 \right] \quad , \tag{A-4}$$

where T_{fi} is the temperature of the liquid at the bubble wall. This is simply a second-order curve which satisfies

$$T(R, t) = T_{fi}$$

$$T(R + \delta \ , \ t) = T_\infty \quad ,$$

and

$$\left(\frac{\partial T}{\partial r}\right)_{r=R+\delta} = 0 \tag{A-5}$$

Here it is convenient for us to define a new variable

$$\gamma_1 \equiv T_\infty - T_{fi} \quad . \tag{A-6}$$

Combining (A-1) and (A-4) with (A-6) and then integrating from R to $R + \delta$, we obtain

$$\frac{1}{\gamma_1} \frac{d\gamma_1}{dt} \left[\frac{1}{3} + \frac{1}{6}\frac{\delta}{R} + \frac{1}{30}\left(\frac{\delta}{R}\right)^2 \right] + \frac{1}{\delta}\frac{d\delta}{dt} \left[\frac{1}{3} + \frac{1}{3}\left(\frac{\delta}{R}\right) + \frac{1}{10}\left(\frac{\delta}{R}\right)^2 \right]$$

$$+ \frac{1}{R}\frac{dR}{dt} \left[\frac{2}{3} + \frac{1}{6}\left(\frac{\delta}{R}\right) \right] = 2\sigma/\rho\delta^2 \quad . \tag{A-7}$$

This differential equation can be greatly simplified by assuming that

$$\delta \ll R \, , \tag{A-8}$$

which is justified later in this appendix. With this simplification Equation (A-7) becomes

$$\frac{2\, d\gamma_1}{\gamma_1} + \frac{2d\delta}{\delta} + \frac{4dR}{R} = \frac{12\alpha}{\delta^2}\, dt \, . \tag{A-9}$$

This equation can be integrated to yield

$$\gamma_1^2 \delta^2 R^4 = 12\, \alpha \int_o^t \gamma_1^2 R^4\, dt \, , \tag{A-10}$$

where $t = 0$ corresponds to the time when

$$R = R_o \, ,$$

$$\delta = 0 \, ,$$

and

$$\gamma_1 = 0 \, . \tag{A-11}$$

We can express the temperature slope at the bubble wall in terms of δ from the assumed temperature distribution in the boundary layer.

$$\left(\frac{\partial T}{\partial r}\right)_{r=R_+} = \frac{2\, \gamma_1}{\delta} \tag{A-12}$$

If we combine this with the boundary condition given by Equation (A-2), we find that

$$\rho_g\, h_{fg}\, \dot{R} = 2\, k_f \gamma_1 / \delta \, . \tag{A-13}$$

Replacing δ in (A-13) from (A-10), we get

$$R^2\,dR = \frac{k_f\,\gamma_1^2\,R^4}{\sqrt{3\alpha}\;\rho_g\,h_{fg}}\left[\int_o^t \gamma_1^2\,R^4\,dt\right]^{1/2} dt\ . \qquad \text{(A-14)}$$

This can be integrated by noting the variable change

$$u_1 \equiv \int_o^t \gamma_1^2\,R^4\,dt\ , \qquad \text{(A-15)}$$

and, therefore,

$$du_1 = \gamma_1^2\,R^4\,dt\ .$$

After integrating and rearranging we obtain

$$\delta = (R^3 - R_o^3)\,\alpha\,\rho_g\,h_{fg}/k_f\,\gamma_1\,R^2\ . \qquad \text{(A-16)}$$

Combining this result with (A-13) we find the desired result to be

$$\dot{R} = 2\,k_b^2\,R^2\,\gamma_1^2/(R^3 - R_o^3)\ , \qquad \text{(A-17)}$$

where the defining equation for k_b is

$$k_b \equiv \frac{k_f}{\rho_g\,h_{fg}\sqrt{\alpha}}\ . \qquad \text{(A-18)}$$

In order for this result to be meaningful, it must be true that

$$\delta/R \ll 1\ . \qquad \text{(A-19)}$$

From (A-16) we can write

$$\delta / R < \frac{\alpha \rho_g h_{fg}}{k_f \gamma_1} \quad , \tag{A-20}$$

and (A-19) can be replaced by the condition that

$$\frac{\alpha \rho_g h_{fg}}{k_f \gamma_1} \ll 1 \, . \tag{A-21}$$

This condition is usually satisfied, especially at low pressures. For instance, water at 50°F gives a value of approximately 10^{-3}.

Satisfying condition (A-21) does not completely justify the use of the integral technique since we have only satisfied the energy equation for the integrated distribution and not at each point in the boundary layer. The integral technique is believed to give a good approximation for the following two reasons:

1. In the limit of large R (asymptotic solution), this technique gives results which are within 2% of the results obtained by Plesset and Zwick [3] and Scriven [5] for the asymptotic region of bubble growth.
2. If a linear temperature profile is used instead of the parabolic one, the results change by only 12%. This indicates the shape of the temperature profile to be relatively unimportant.

APPENDIX B

Simplification of Mass Flux Equation

The irreversible mass flux (Equation (15)) can be written as

$$\dot{R} = \frac{- L_{ii} P v_{fg}}{\rho_g T} \left[- \frac{K}{K+1} \frac{h_{fg}}{P v_{fg}} \frac{\partial T}{T} + \frac{\partial_f P}{P} \right] , \tag{B-1}$$

where the notation is the same as in the body of this paper. The purpose here is to show that the first term in the brackets is very small compared to the second.

This is accomplished by noting that the slope of the vapor temperature profile at the bubble wall starts out as negative and remains negative throughout bubble growth. The profile starts out negative because the temperature at the bubble wall decreases much faster due to latent heat requirements than does the bulk temperature of the vapor due to the work of the pressure forces. To show this, we calculate the order of magnitude of the mean temperature decrease inside the bubble when the bubble volume doubles from its initial unstable equilibrium state. For this change the work is

$$\delta Wk = P\,\delta V \approx \frac{m_b\,\bar{R}T}{V_o}\,\delta V \approx m_b\,\bar{R}T\,, \tag{B-2}$$

where m_b is the initial mass of vapor in the bubble. The corresponding change in the average temperature T_m of the vapor must be

$$\delta T_m = \frac{m_b\,\bar{R}T_m}{c_v} \tag{B-3}$$

We form a ratio by dividing by ΔT_s and use the perfect gas law to obtain

$$\frac{\delta T_m}{\Delta T_s} = \frac{P_\infty\,V_o}{c_v \Delta T_s}\,. \tag{B-4}$$

This ratio is extremely small. For example, water at $50^{\circ}F$ gives a value of about 10^{-12}.

The corresponding decrease in the wall temperature can be shown to be much larger than δT_m. In Appendix A it was found that

$$\dot{R} = \frac{2 k_b^2 R^2}{R^3 - R_o^3} \gamma_1^2 \quad . \tag{B-5}$$

Now we want to find the value for γ_1 when the bubble volume has doubled. This is approximately given by

$$\gamma_1^2 \approx \frac{\dot{R} R_o}{2 k_b^2} \quad , \tag{B-6}$$

or using the definition of the dimensionless velocity, we find that

$$\frac{\gamma_1}{\Delta T_s} \approx \sqrt{\hat{R}} \quad , \tag{B-7}$$

which for water at $50^{\circ}F$ is approximately 10^{-1}; therefore, it must be true, during early bubble growth, that the slope of the temperature profile in the vapor is negative. As growth continues the slope will tend toward zero because energy is conducted away from the bubble, and at the same time the vapor flux coming into the bubble is at a temperature lower than the bulk temperature of the vapor in the bubble. In summary we concluded that the slope of the temperature in the vapor at the bubble wall must always be negative.

Using this fact we can show that the temperature discontinuity across the interface is always smaller than a given quantity δT_{max}. We shall then proceed to show that δT_{max} is small.

The energy flux into the bubble at the bubble wall can be expressed as

$$J_u = h_g J_i + k_g \left(\frac{\partial T}{\partial r}\right)_{r=R_-} , \tag{B-8}$$

or, by using the irreversible energy flux, as

$$J_u = \frac{1}{K+1}\left[K h_f + h_g \right] J_i - L_k \frac{\delta T}{T^2} . \tag{B-9}$$

Combining (B-8) and (B-9) we get

$$k_g \left(\frac{\partial T}{\partial r}\right)_{r=R_-} = \frac{-K h_{fg} J_i}{K+1} - L_k \frac{\delta T}{T^2} . \tag{B-10}$$

From (B-10) we see that δT will have its largest absolute value when $k_g(\partial T/\partial r)_{r=R_-}$ has its largest algebraic value, which was shown above to be zero. Thus it follows that

$$\frac{\delta T_{max}}{T} = -\left(\frac{K}{K+1}\right) \frac{h_{fg} T}{L_k} J_i . \tag{B-11}$$

Substituting in (B-11) for J_i we find that

$$\xi = \left[1 + \left(\frac{K+1}{K}\right)^2 \frac{L_k}{h_{fg}^2 L_{ii}} \right]^{-1} , \tag{B-12}$$

where we have defined ξ as

$$\xi \equiv \frac{(K/K+1)(h_{fg}/Pv_{fg})(\delta T_{max}/T)}{(\delta P/P)} \tag{B-13}$$

The quantity ξ has been defined so that it is the ratio of the terms which add in Equation (B-1). In other words we need to show ξ to be small. Anticipating ξ to be a small number, we can simplify (B-12) as

$$\xi \approx \frac{K^2}{(K+1)^2} \frac{h_{fg}^2 L_{ii}}{L_k} \quad . \tag{B-14}$$

Now if we substitute in (B-14) the approximate kinetic theory values for $K/(K+1)$, L_{ii}, and L_k and use the perfect gas law, we find that

$$\xi \approx \frac{2 \sigma_c}{2 - \sigma_c} \frac{(\gamma - 1)}{(\gamma + 1)\, 4} \quad , \tag{B-15}$$

or since

$$\sigma_c \leq 1 \ ,$$

that

$$\xi \leq \frac{(\gamma - 1)}{2(\gamma + 1)} \quad . \tag{B-16}$$

The right-hand side of (B-16) is approximately 10^{-1} indicating that the term we neglected is at least one order of magnitude smaller than the other term in Equation (B-1).

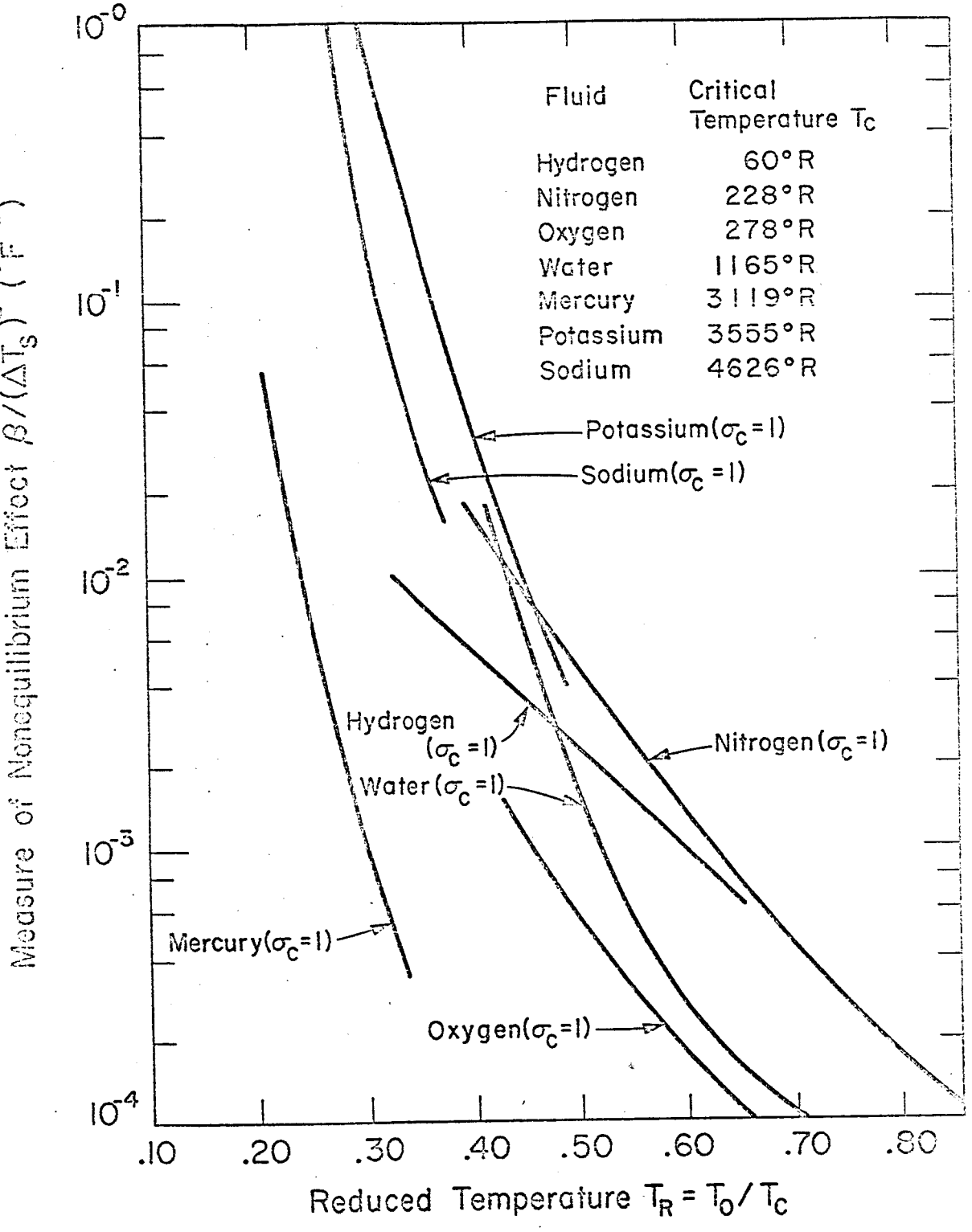

Fig. 1 Dimensionless Fluid Parameter β Versus Reduced Temperature

Fig. 1 Bernhurst and Hatsopoulos

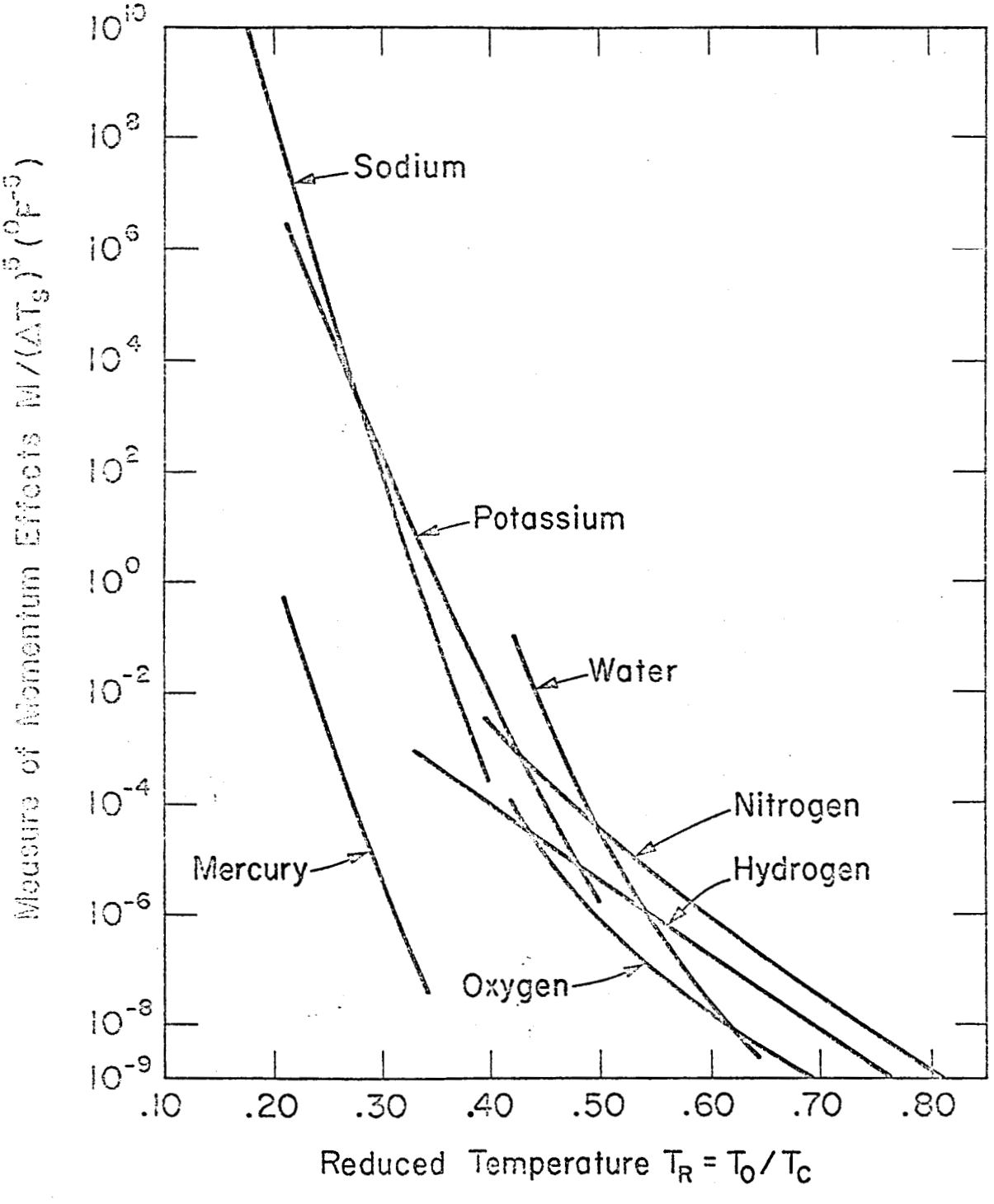

Fig. 2 Dimensionless Fluid Parameter M Versus Reduced Temperature

Fig. 2 — Bernhorst and Hatzopoulos

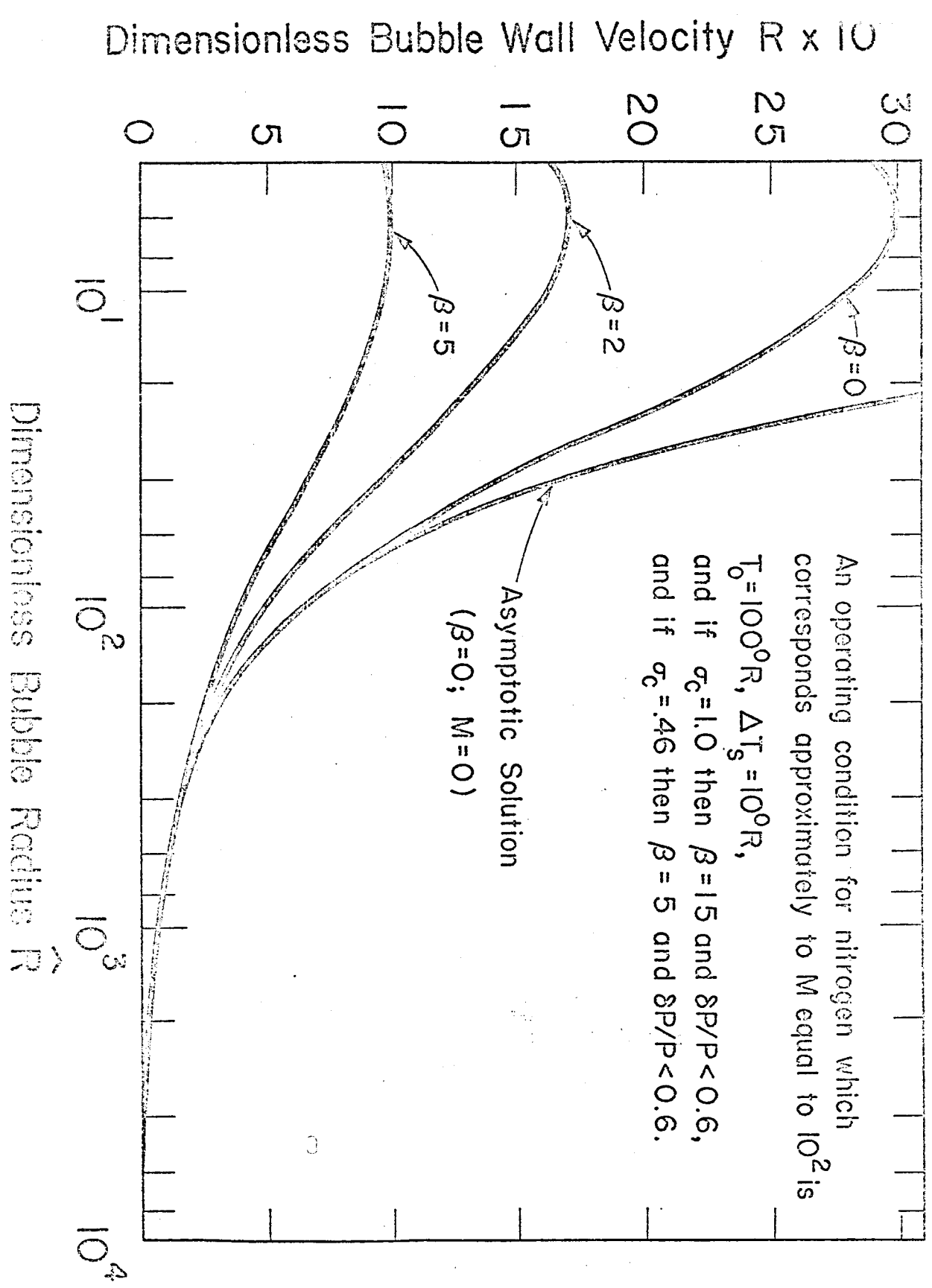

Fig. 3 Dimensionless Bubble Wall Velocity Versus Dimensionless Bubble Radius with M Equal to 10^2

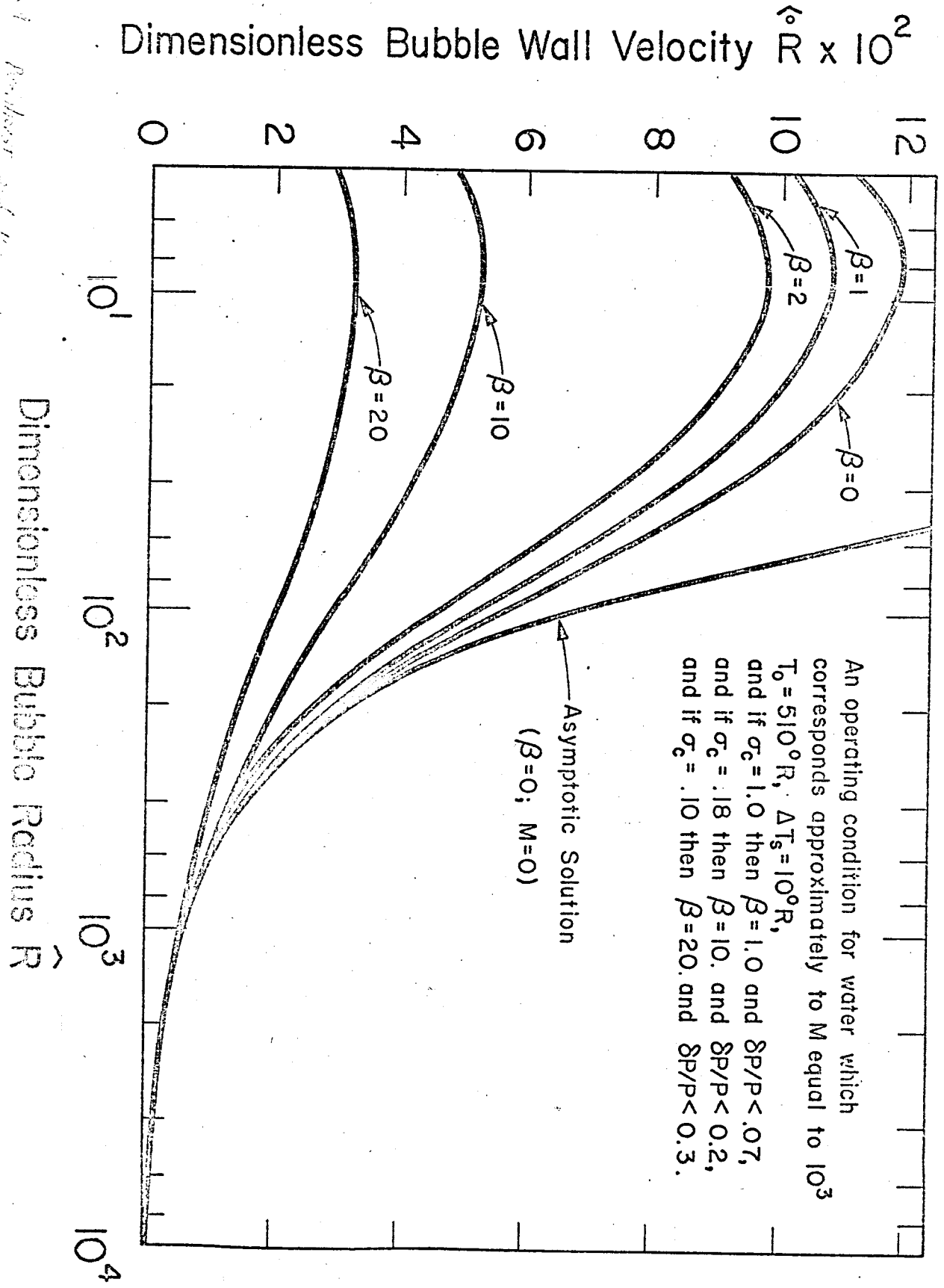

Fig. 4 Dimensionless Bubble Wall Velocity Versus Dimensionless Bubble Radius with M Equal to 10^3

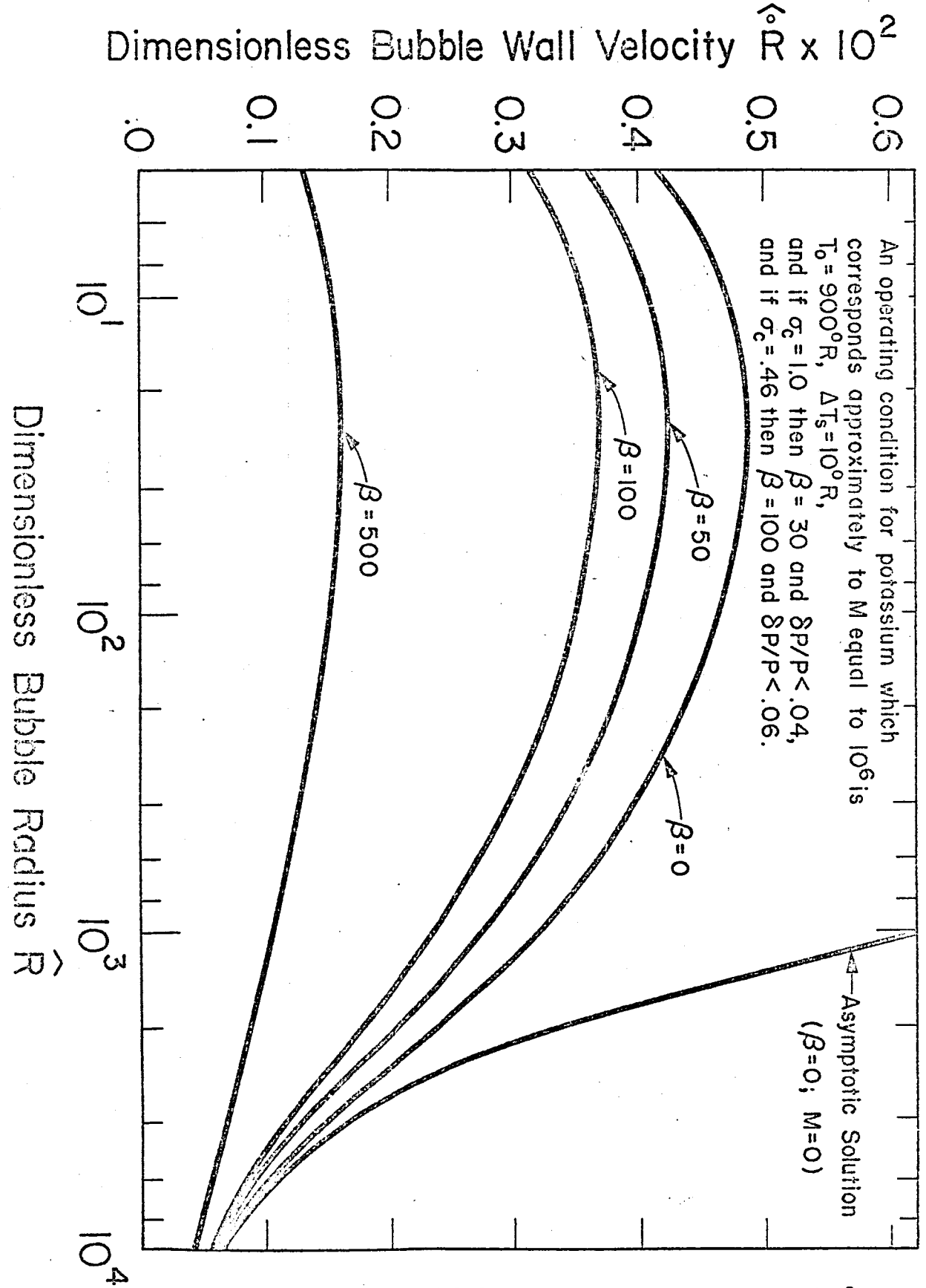

Fig. 5 Dimensionless Bubble Wall Velocity Versus Dimensionless Bubble Radius with M Equal to 10^6

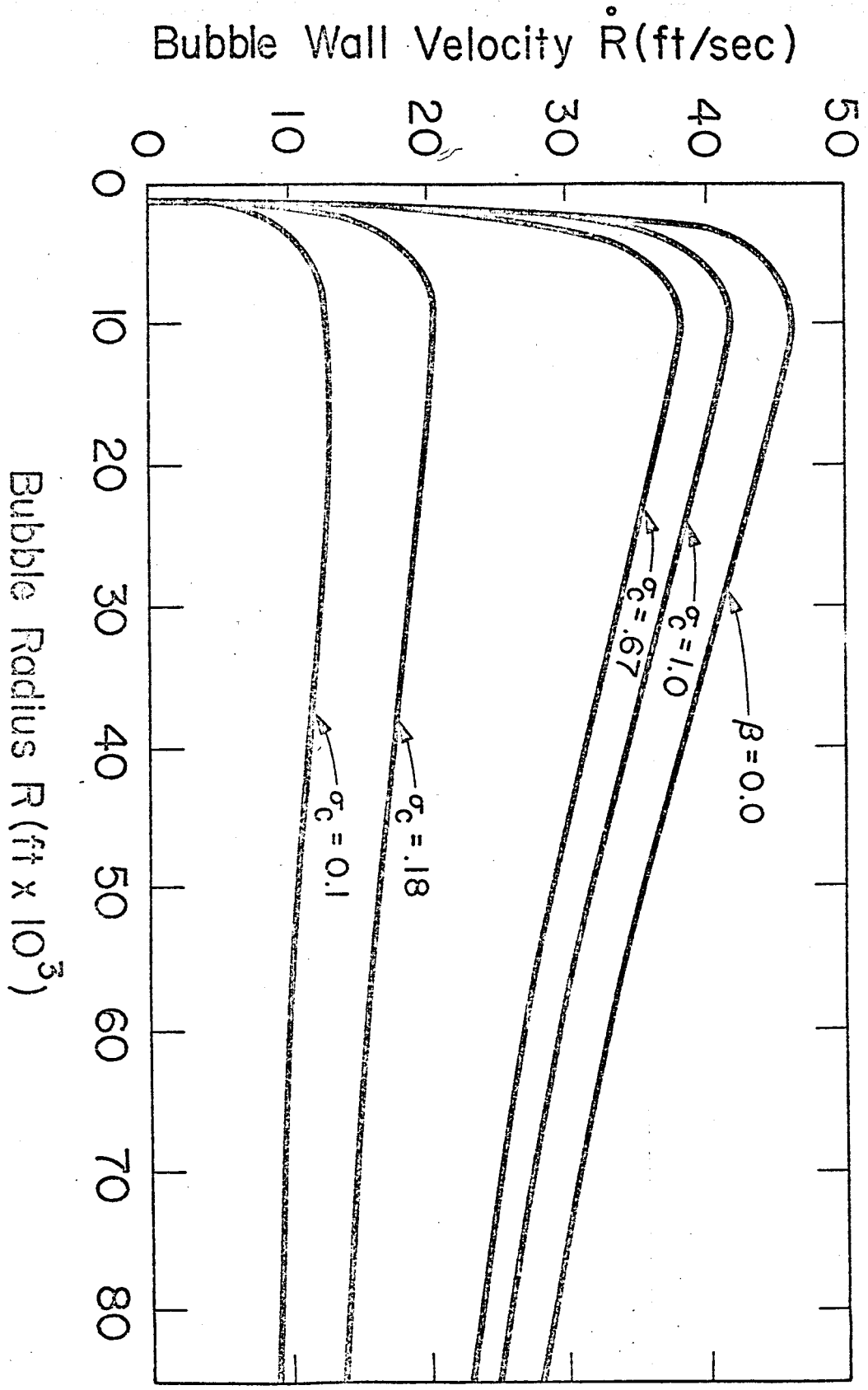

Fig. 6 Bubble Wall Velocity Versus Radius for Water with T_o Equal to 50 °F and ΔT_s Equal to 10 °F